Neuropsychologia 128 (2019) 127–139

Contents lists available at ScienceDirect

Neuropsychologia

journal homepage: www.elsevier.com/locate/neuropsychologia

Visually evoked responses from the blind field of hemianopic patients

Javier Sanchez-Lopez[a,*], Caterina A. Pedersini[a], Francesco Di Russo[b,c], Nicolò Cardobi[a], Cristina Fonte[d], Valentina Varalta[d], Massimo Prior[e], Nicola Smania[d], Silvia Savazzi[a,f,g], Carlo A. Marzi[a,g]

[a] Department of Neuroscience, Biomedicine and Movement, University of Verona, Italy
[b] Department. of Movement, Human and Health Sciences, University of Rome "Foro Italico", Rome, Italy
[c] IRCCS Santa Lucia Foundation, Rome, Italy
[d] Neuromotor and Cognitive Rehabilitation Research Center, Department of Neuroscience, Biomedicine and Movement, University of Verona, Italy
[e] ASL 8 Asolo, Treviso, Italy
[f] Perception and Awareness (PandA) Laboratory, Department of Neuroscience, Biomedicine and Movement, University of Verona, Italy
[g] National Institute of Neuroscience, Verona, Italy

ARTICLE INFO

Keywords:
Hemianopia
Steady-state visual evoked potentials
Extrastriate visual areas
Perceptual awareness

ABSTRACT

Hemianopia is a visual field defect characterized by decreased vision or blindness in the contralesional visual field of both eyes. The presence of well documented above-chance unconscious behavioural responses to visual stimuli presented to the blind hemifield (blindsight) has stimulated a great deal of research on the neural basis of this important phenomenon. The present study is concerned with electrophysiological responses from the blind field. Since previous studies found that transient Visual Evoked Potentials (VEPs) are not entirely suitable for this purpose here we propose to use Steady-State VEPs (SSVEPs). A positive result would have important implications for the understanding of the neural bases of conscious vision. We carried out a passive SSVEP stimulation with healthy participants and hemianopic patients. Stimuli consisted of four black-and-white sinusoidal Gabor gratings presented one in each visual field quadrant and flickering one at a time at a 12 Hz rate. To assess response reliability a Signal-to-Noise Ratio analysis was conducted together with further analyses in time and frequency domains to make comparisons between groups (healthy participants and patients), side of brain lesion (left and right) and visual fields (sighted and blind).

The important overall result was that stimulus presentation to the blind hemifield yielded highly reliable responses with time and frequency features broadly similar to those found for cortical extrastriate areas in healthy controls. Moreover, in the intact hemifield of hemianopics and in healthy controls there was evidence of a role of prefrontal structures in perceptual awareness. Finally, the presence of different patterns of brain reorganization depended upon the side of lesion.

1. Introduction

A lesion along the central visual pathway (from optic tract to visual cortex) often yields specific visual defects characterized by decreased vision or blindness of the contralesional visual field of both eyes, i.e. homonymous hemianopia (see Bouwmeester et al., 2007). In some cases, usually as a result of lesion of the optic radiation, the visual field defect may be limited to the upper or lower quadrant (quadrantanopia). More rarely, as a result of bilateral damage, a loss of vision of the superior or the inferior half of both visual hemifields may occur (altitudinal hemianopia). Thanks to the "revolutionary" discovery of Poppel et al. (1973) and Weiskrantz et al. (1974) of the existence of unconscious visually triggered responses, hemianopic patients have become a fundamental source of information on the neural mechanisms of visual perceptual awareness and on possible mechanisms of recovery from cortical blindness. Larry Weiskrantz defined as "blindsight" unconscious visually triggered behavior which was later subdivided into Type I and Type II according to the absolute lack of any form of perceptual awareness or to the presence of a "feeling" that a visual stimulus was presented, respectively (Weiskrantz, 1997). The study of the neural substrate of blindsight is obviously of crucial importance to understand the mechanisms enabling perceptual awareness. So far there have been several functional magnetic resonance imaging (fMRI) studies (see Ajina et al., 2015; Bridge et al., 2010). Their contribution has provided important information but the temporal dynamics of the shift from unconscious behavior to blindsight of either Type I or II and

* Correspondence to: Department of Neuroscience, Biomedicine and Movement, University of Verona, Istituti Biologici 2 Piano, Strada le Grazie 8, 37134, Verona, Italy.
E-mail address: javier.sanchezlopez@univr.it (J. Sanchez-Lopez).

http://dx.doi.org/10.1016/j.neuropsychologia.2017.10.008
Received 16 August 2017; Received in revised form 2 October 2017; Accepted 3 October 2017
Available online 05 October 2017

possibly to full recovery of perceptual awareness require a much higher temporal resolution than fMRI, such as that ensured by electroencephalographic (EEG) methods.

Visual evoked potentials (VEPs) represent an EEG technique that measures variation of cortical activity as a function of time or frequency during repeated visual stimulation and can provide detailed information on the functional status of the visual system. Transient VEPs are the most used technique and are produced by slow-rate stimulus presentation (below 4 Hz) to allow the brain activity evoked by a stimulus to return to baseline level before the next stimulus is delivered. Transient VEPs have been frequently used not only in basic visual neurophysiology but also for the diagnosis of several optical and neurological pathologies. However, their use in the study of hemianopic patients has been very scanty albeit with some exceptions (Brecelj, 1991; Celesia and Brigell, 1999; Ffytche et al., 1996; Kavcic et al., 2015; Rossion et al., 2000; Schomer and Lopes da Silva, 2011). Shefrin et al. (1988) were the first to study the neural correlates of blindsight in hemianopic patients but found that visual stimuli (words) presented to the blind hemifield could not elicit a response except for one patient with clinical signs of blindsight out of four patients tested. This patient showed task-related late activity such as the P3 and some earlier components around 80–300 ms. They concluded that the kind of blindsight shown was not mediated by the geniculo-striate pathway. In keeping with this conclusion, early components peaking around 90–130 ms after stimulus onset have been found in later studies in healthy participants to arise from extrastriate visual areas (e.g. Di Russo et al., 2016). Furthermore, Kavcic et al. (2015) with moving visual stimuli did find VEP responses to stimulus-onset presentation from the damaged hemisphere but only when the intact hemifield was stimulated and therefore via interhemispheric connections. Interestingly, with motion-onset stimuli, VEP responses could be obtained only from patients with left hemisphere damage. Broadly similar results have been observed by Bollini et al. (2017) who studied the VEP responses to static and moving stimuli in two hemianopic patients with either right or left occipital lesion. Results clearly showed the presence of N1 and P2 components over the damaged hemisphere for both static and moving stimuli, and a late negative component (around 350 ms) in the intact hemisphere but only for moving stimuli and when stimulating the blind hemifield in the left lesioned patient who also showed blindsight. Authors suggested that interhemispheric transfer mechanisms subserved this kind of blindsight for moving stimuli.

Given this relatively scanty evidence, in the present study we decided to use another type of VEP, namely, steady-state VEPs (SSVEPs) where repetitive (or flickering) visual stimuli are presented at a high rate (usually from 10 to 20 Hz), eliciting a continuous and steady sequence of oscillatory potential changes arising mainly in the visual cortex. This stimulation is rapid enough to prevent the evoked neural activity from returning to baseline. The SSVEPs reflect high propagation properties (i.e. a combination of locally and widely temporally distributed sources), are less sensitive to different kinds of artifacts, require much less time to acquire data and have a larger signal-to-noise ratio (SNR) than transient VEPs (Di Russo et al., 2002b; Vialatte et al., 2010).

To our knowledge, no evidence is available on SSVEP responses from the blind field of hemianopic patients. Thus, the present study was motivated by the idea that SSVEP might be sensitive enough to record residual functional activity from cortical visual areas in the lesioned or the intact hemisphere following stimulus presentation to the blind hemifield.

The SSVEP generally appears in scalp recordings as a near-sinusoidal waveform at the frequency of the driving stimulus and its harmonics i.e. the waveforms are typically modulated at the fundamental stimulus frequency in the case of an unstructured stimulus (e.g. flash) or at the double of the fundamental frequency if the stimulus is a contrast-reversing pattern (e.g. checkerboard or sinusoidal grating, Regan, 1989). It can be measured in time, frequency and time-frequency domains and is better observed in frequency or time-frequency (Schomer and Lopes da Silva, 2011; Vialatte et al., 2010). Previous SSVEP studies, combined with fMRI in healthy participants have found that repetitive 6 Hz pattern-reversal stimulation produces a sequence of oscillatory brain potentials at 12 Hz (i.e. the second harmonic) with activations located over the primary visual cortex (V1), motion sensitive brain areas (MT/V5) mid-occipital (V3A) and ventral occipital (V4/V8) areas (Di Russo et al., 2007).

Accordingly, the specific objectives of the present study are to evaluate the reliability of SSVEP elicited by stimulation of the blind field of hemianopic patients, and to describe the time and frequency modulations and the spatial distribution of this activity. The more general aim is to try and understand the neural mechanism of the possible shift from loss of visual perceptual awareness to unconscious above chance visual behavior (see Weiskrantz, 1996) and possibly to recovery of conscious vision. To achieve that, one important initial step is to find out whether one can demonstrate the presence of reliable neural visual responses following presentation of visual stimuli to the blind field of hemianopic patients not only those exhibiting blindsight but also those in which it was not possible to demonstrate unconscious above chance visually triggered behavior. To anticipate the major finding described below, we were amazed to find out that all hemianopic patients, with or without blindsight, showed reliable responses to visual stimuli presented to the blind hemifield.

2. Material and methods

2.1. Participants

Thirteen young healthy participants (10 females; mean age = 27.2 years old, SD = 3.0), and thirteen hemianopic patients (4 females; mean age = 58.0 years old, SD = 9.1) with different long-standing post-chiasmatic lesions participated in the study. According to the inclusion criteria, only patients with hemianopia diagnosed at least three months before the first testing session and who had undergone clinical visual campimetry and structural MRI were included. The criteria for exclusion were: pre-existing neurologic or psychiatric disorders, drugs or alcohol addiction, presence of a general cognitive impairment as revealed by a score equal or less than 24 at the Mini Mental State Examination (Folstein et al., 1975) and presence of impairment of spatial attention (i.e. hemineglect). The presence of the last impairment was tested with a neuropsychological battery including: Line Bisection (Schenkenberg et al., 1980), Diller letter H cancellation (Diller et al., 1974) and Bell Cancellation (Gauthier et al., 1989). Finally, patients were evaluated with the Visual Function Questionnaire (VFQ25) in order to assess their subjective impressions on their visual abilities in everyday life (Mangione et al., 1960). All healthy participants and patients had normal or corrected to normal visual acuity. Informed consent was obtained from healthy participants and patients after they had been fully informed about the experimental procedures and their rights. The study was approved by the Ethics Committee of the European Research Council and of the Verona Azienda Ospedaliera Universitaria Integrata (AOUI).

Summary of the clinical details of the patients are detailed in Table 1. Patients' clinical campimetry is shown in Fig. 1 and cerebral lesions are in Fig. 2.

2.2. Stimuli

The visual stimulus (see also Di Russo et al., 2007) consisted of a circular black and white horizontal Gabor grating whose diameter was 2° of visual angle and with a spatial frequency of 4c/° (see Fig. 3). The background luminance (18 cd/m^2) was the same as the mean luminance of the Gabor grating which was contrast modulated at 32%. The flickering of the grating was obtained by contrast reversal each 83.3 ms (i.e. a reversal rate of 12 Hz) to complete a cycle every 166.7 ms

Table 1
Patients' clinical details.

Patient	Age	Post-Damage Interval (months)	Gender	Lesion	Hemianopia
LF	50	40	F	Ischemic lesion that involves the cortex of the anterior half of right calcarine fissure to the origin of parieto-occipital fissure.	Upper left quadrantanopia.
AP	47	47	M	Lesion involving the inferior anterolateral portion of right occipital lobe with extension in the posterior part of the temporal lobe and the upper part of right cerebellar hemisphere. A partial sparing of calcarine fissure was present.	Upper left quadrantanopia.
RC	50	9	M	Lesion involving the medial portion of right occipital lobe. There is an involvement of the lingual and fusiform gyri till the occipital pole, with alterations of the calcarine fissure, especially the inferior part.	Upper left quadrantanopia.
BC	69	10	M	Lesion involving the medial portion of right occipital lobe, with an extension over the parieto-occipital fissure. An important involvement of the lingual and fusiform gyri till the occipital pole, with alterations of the calcarine fissure is observed.	Left lateral hemianopia.
GS	75	9	M	Lesion involving the antero-superior part of the right calcarine fissure with relative sparing of the posterior part. A partial involvement of the cuneus is observed.	Left lateral hemianopia.
LC	66	9	M	Right temporal and parietal lesion, with posterior extension to the white matter of occipital lobe, involving the lateral part of optic radiation. The right calcarine fissure is normal.	Left lateral homonymous hemianopia.
FB	49	17	F	Extensive lesion mainly involving the right temporal and parietal lobe, with development of a poro-encephalic cavity in temporal lobe and ex-vacuo dilatation of right lateral ventricle. In the occipital lobe, the lesion involves the superior and a portion of the middle occipital gyri. Right optic radiation was interrupted. The other parts of occipital lobe are preserved.	Left lateral homonymous hemianopia.
HE	60	7	M	Lesion involving the medial part of right occipital lobe with *peri*-calcarine distribution. The alterations are predominately in the upper part of calcarine fissure with extension to the cuneus.	Left lateral homonymous hemianopia.
GA	60	15	M	Ischemic lesion involving the left parieto-occipital lobe. In the occipital lobe, laterally, the lesion involves the superior, middle, inferior and descending occipital gyri. Medially the lesion involves the cuneus and the occipital pole and the white matter of the posterior part of optic radiation, with relative sparing of the lingual and fusiform gyri.	Lower right quadrantanopia.
SL	47	70	F	Lesion involving the median para-sagittal portion of the left occipital lobe. The lesion involves the lingual gyrus, with *peri*-calcarine fissure distribution.	Right lateral homonymous hemianopia.
AN	54	29	M	Lesion involving the left temporo-parietal lobe, with extension to the occipital lobe in the superior and middle occipital gyri. The alteration of the white matter in the occipital lobe suggests an involvement of the upper part of left optic radiation.	Right lateral homonymous hemianopia.
LB	62	5	F	Ischemic lesion in the vascular territory of the left posterior cerebral artery, involving the entire occipital lobe, including the left calcarine fissure.	Right lateral homonymous hemianopia.
AM	65	38	M	Bilateral median para-sagittal occipital ischemic lesions involving the lingual gyrus, more evident in the right side. On the right side, a thinning of the anterior portion of calcarine cortex is observed.	Bilateral Altitudinal Hemianopia.

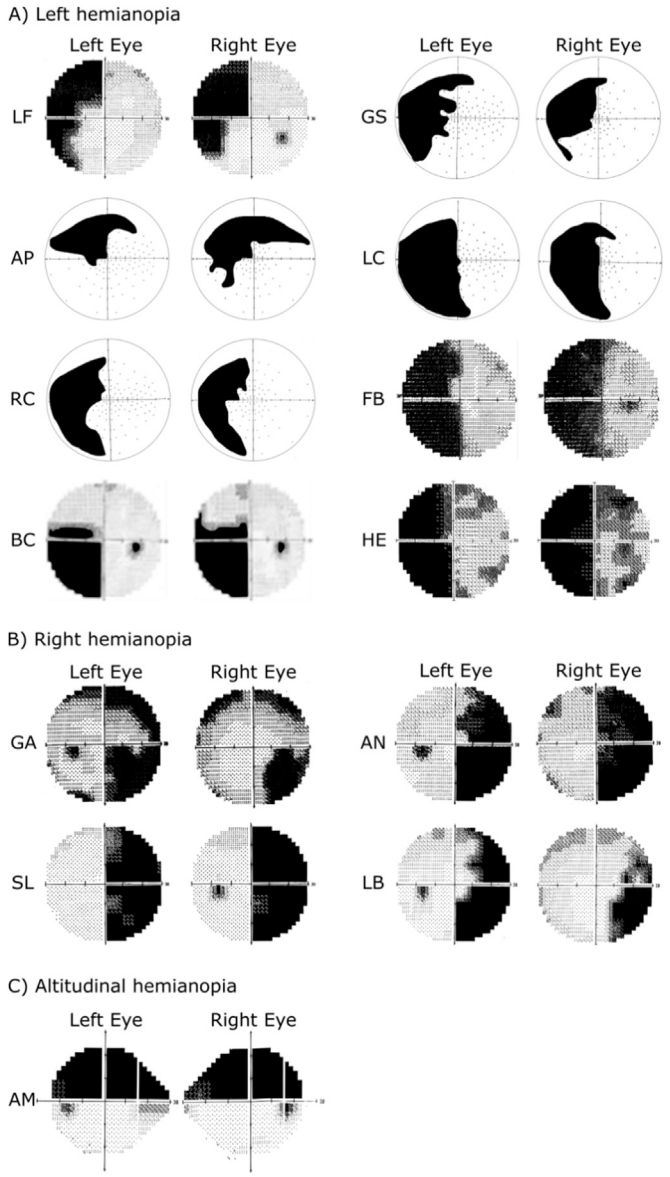

Fig. 1. Patients' clinical campimetry A) left hemianopia (right hemisphere lesion); B) right hemianopia (left hemisphere lesion) and C) bilateral altitudinal hemianopia (bilateral hemispheric lesion). Humphrey Field Analyzer II (HFA) visual perimetries used are: SITA-standard strategy for patients LF, FB, BC, HE, GA, AN, SL, LB and AM; and two zone strategy for GS, AP, LC and RC. Descriptions of the lesions are reported in Table 1.

(fundamental frequency of 6 Hz). The stimulation was performed by presenting simultaneously four sinusoidal Gabor gratings on the screen each on one of the four quadrants of the visual field: upper right, upper left, lower right and lower left.

2.3. SSVEP stimulation

Participants were comfortably seated in front of a LCD video monitor (resolution = 1920 × 1080; refresh rate = 144 Hz) at a viewing distance of 57 cm from the monitor screen. The stimuli were binocularly presented and participants were asked to maintain a stable fixation on a central cross during stimulus presentation. Ocular movements were externally controlled through a close-circuit camera and constant feedback about their ability to maintain fixation was given. SSVEP stimulations consisted of 4 runs that included 12 blocks of 20 s of flickering each (240 s of stimulation for run). Short breaks were included between blocks and longer pauses between runs. Each block consisted of the presentation of the four Gabor stimuli described above (one in each quadrant of the visual field); during stimulus presentation each Gabor grating started flickering one at a time for 5 s with inter-stimulation intervals of 400 ms. The presentation of the flickering Gabor was randomized across quadrants and a total of 2800 pattern-reversal stimuli for each quadrant was obtained.

For each patient the stimulus was positioned in the blind area on the basis of the results of the clinical campimetry (see Fig. 1) and of a visual mapping test carried out in the lab. This testing had two purposes: a) to determine for each patient the blind portion of the visual field with a binocular stimulus presentation in the same experimental conditions as in the subsequent experiment; and b) to train patients to keep the gaze steadily on the fixation point at the center of the screen by controlling eye movements through a close-circuit camera and an eye-tracking system (The EyeTribe ©). For visual mapping 2° square-wave gratings with 7 bars and Michelson contrast of 1 were used. Background mean luminance was 4.15 cd/m2. Stimuli were presented on the screen with exposure duration of 150 ms in a pseudo-random order at different eccentricities (more often in the blind field). Patients were comfortably seated in front of a LCD video monitor at a viewing distance of 57 cm in a dimly lit room and were instructed to press the space bar of a keyboard as quickly as possible following detection of the stimulus. For patients with a full hemianopic loss, stimuli were presented three times randomly in 195 positions in the blind field and 20 in the sighted field, whereas for patients with quadrantanopia they were presented in 91 positions in the blind and 10 in the sighted field. Data were processed in MATLAB (version 8.2.0, The MathWorks, Inc., Natick, MA, 2010) to generate a greyscale map of the visual field with different shades of gray, see Fig. 4 for an example of visual map. Maps were compared to the patients' clinical campimetry to confirm the extension of the visual field and select the best position to present the stimuli in the blind field and in the corresponding intact field on the opposite side. Eccentricities of stimulus presentation for each patient are reported in Table 2. For healthy participants stimulus position was the same for the whole group (see Fig. 3).

2.4. EEG recording

EEG was recorded from 59 active electrodes (ActiCap, Brain Products GmbH, Munich Germany) placed according to the 10-10 International System with two BrainAmp amplifiers and acquired using the Recorder 1.2 (Brain Products GmbH, Munich, Germany). The left mastoid served as on-line reference; additionally the right mastoid electrode was used in order to re-reference recording offline to the average of the right and left mastoid electrodes. The ground electrode was placed at the AFz electrode position. Horizontal and vertical eye movements were monitored with four electrodes placed at the left and right canthi and above and below the right eye, respectively. The impedance of all electrodes was kept below 5 KΩ. The EEG was recorded at 1000 Hz sampling rate with a time constant of 10 Hz as low cut-off and a high cut-off of 1000 Hz with a 50 Hz notch filter.

2.5. Analysis

2.5.1. EEG pre-processing

The EEG signal was pre-processed offline using Analyzer 2.1 software (Brain Products GmbH, Munich, Germany), MATLAB (version 8.2.0, The MathWorks, Inc., Natick, MA, 2010) scripts and EEGLAB toolbox (Delorme and Makeig, 2004). Firstly, data pre-processing was carried out for all channels by re-referencing to the average of the right and left mastoid electrodes. Vertical eye movements were corrected by means of Independent Component Analysis (ICA) ocular correction (Makeig et al., 1996), a method that consists of separating the EEG signal into maximally independent components allowing semi-automatically the removal of ocular artefacts. Continuous EEG recording was segmented into 2 s overlapped epochs of all conditions corresponding to the four quadrants (upper left, upper right, lower left and lower right); all segments were

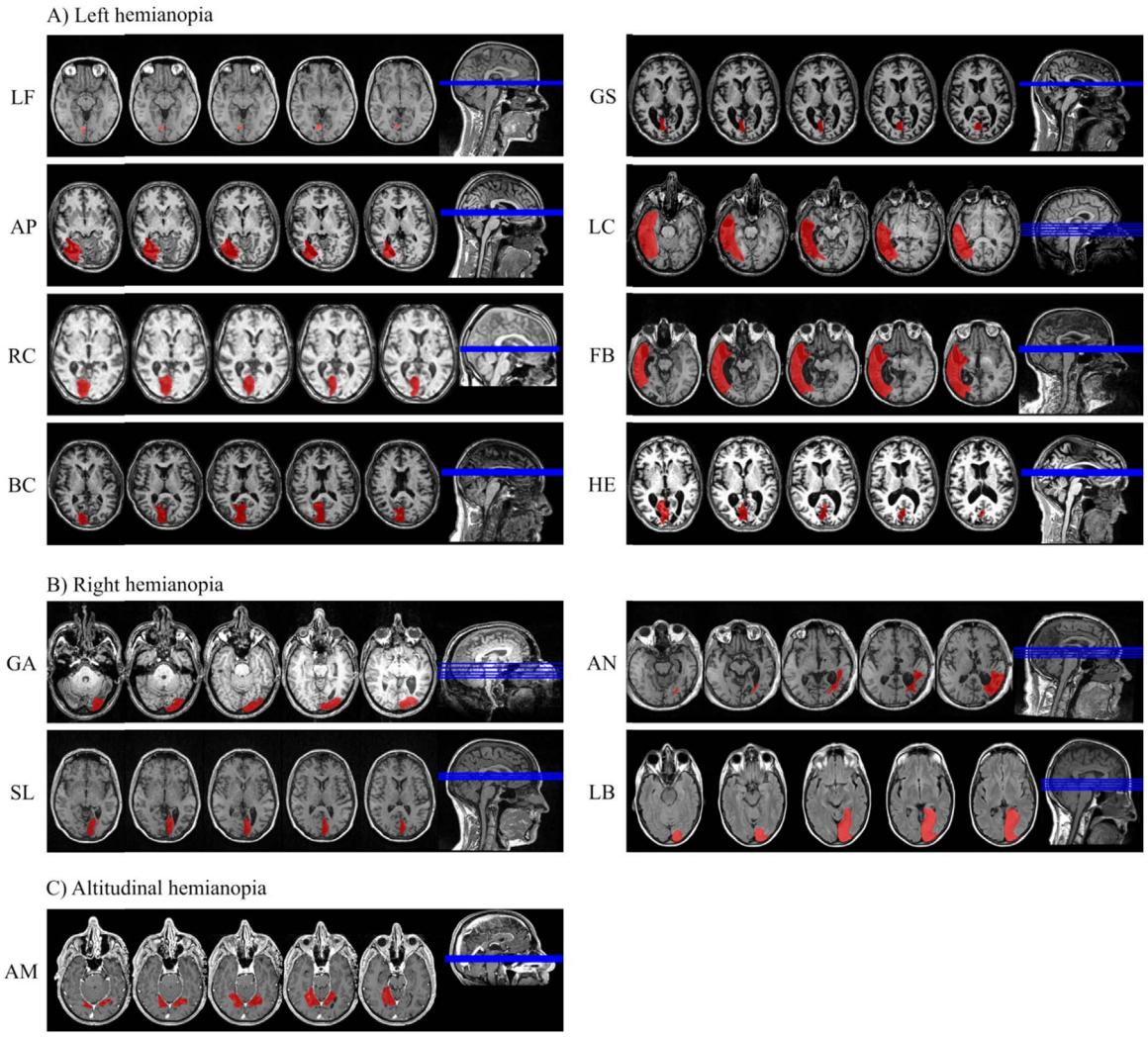

Fig. 2. Patients' structural magnetic resonance images. Localization and extension of the lesions are drawn in red. A) right hemisphere lesion with resulting left hemianopia; B) left hemisphere lesion with resulting right hemianopia; and C) bilateral hemispheric lesion with resulting bilateral altitudinal hemianopia. Images are left-right oriented according to the radiological convention.

band pass filtered from 5 to 40 Hz. Baseline correction was performed for each segment by removing the mean value of the signal per channel per trial. Finally, semiautomatic rejection of segments with artefacts was carried out by removing segments with voltages upper and lower ± 80 μV, and with muscle artefacts and horizontal eye movements. On average, about 10% of the segments were rejected. Clean segments obtained from each quadrant were separately averaged and 12 Hz modulated waveforms were obtained. Finally, the power of frequency, by means of the fast Fourier transformation (FFT), was extracted at each channel of the averaged SSVEP as 2 s segments.

2.5.2. Signal reliability (SNR)

The SNR, was calculated by means of the rhythmic entrainment source separation (RESS) method (for a full explanation see Cohen and Gulbinaite, 2017). RESS consists of linear spatial filters which multiply the EEG electrode time series to produce a weighted combination of all the electrodes instead of the data from individual electrodes and therefore performing a temporally filtered generalized eigendecomposition of selected covariance matrices, a signal covariance matrix (*S*) filtered at the SSVEP frequency and a "reference" or noise covariance matrix (*R*) filtered at frequencies neighbouring the SSVEP which can boost the SNR of the SSVEP. For our data, the *S* matrix was computed at 12 Hz while the *R* matrices were computed at ± 1 neighbours frequencies (i.e. 11 and 13 Hz), and SNR values were obtained for each frequency per condition per participant. To assess the difference between SNR values of the signal (12 Hz) and the reference or noise (11 and 13 Hz) an ANOVA was performed with group (patients and healthy participants) as between-subjects factor, quadrant of stimulation (upper left, upper right, lower left and lower right) and frequency (11, 12 and 13 Hz) as within-subject factors. Additionally, blind and intact fields, in the patients group, were separately analysed by selecting one blind and one intact quadrant for each patient and performing two different ANOVAs with frequency (11,12 and 13 Hz) as within-subject factor. The Greenhouse-Geisser epsilon was applied to correct the degrees of freedom of the F-distribution. Post-hoc analyses were performed using the Bonferroni correction.

2.5.3. Time and frequency analysis

2.5.3.1. Time. To make a general comparison between patients and controls one single group of patients was formed by flipping left-right the brain electrical activity of patients with left hemisphere lesion. Thus, **patients** were divided in four groups according to the (upper or lower) position of their blind field and the corresponding intact field: upper blind field (n = 12; LF, AP, RC, BC, GS, LC, FB, HE, SL, AN, LB, AM), lower blind field (n = 10; RC, BC, GS, LC, FB, HE, GA, SL, AN, LB), upper sighted field (n = 12; LF, AP, RC, BC, GS, LC, FB, HE, GA, SL, AN, LB), and lower sighted field (n = 13; LF, AP, RC, BC, GS, LC, FB, HE, GA, SL, AN, LB, AM). In the **healthy group** all the four quadrants of stimulus presentation were considered. For this first

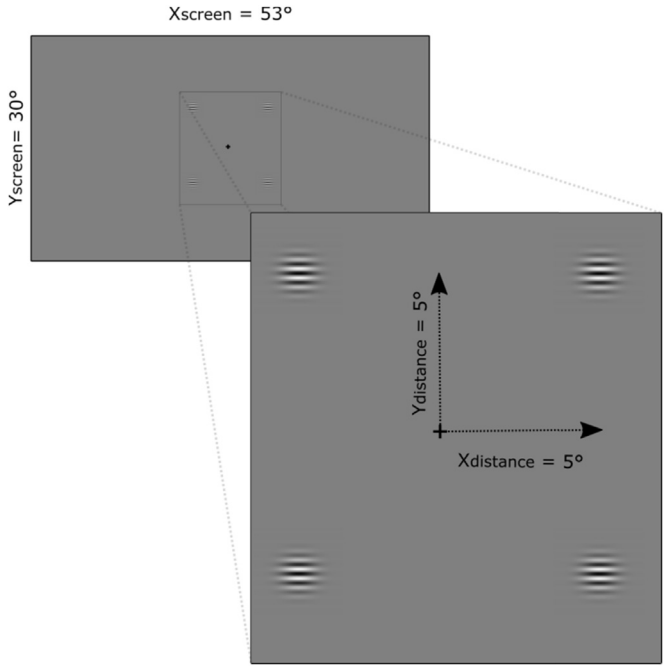

Fig. 3. Eccentricities of the stimuli for healthy participants.

descriptive analysis we adopted a procedure similar to that of Di Russo et al. (2007) with healthy participants. To visualize the temporal SSVEP modulation, grand-average waveforms were constructed for each condition in both patients and healthy groups.

2.5.3.2. Frequency. Analyses consisted of three steps to assess descriptively as well as statistically the frequency modulation related to the presence and the side of the visual field loss in the patients group. To do that, data were analysed by forming groups of patients according to the blind and sighted quadrants and the side of lesion (left or right). The procedure for these analyses is described below.

2.5.3.2.1. Step 1: General overview in hemianopic patients. The aim of this step was to evaluate general differences and similarities in frequency modulation over occipital electrodes between healthy participants and patients. As in the previous analysis, the activity of left lesioned patients was flipped left-right and a group of 9 patients (those with quadrantanopia were not included in this analysis) was formed and

Table 2
Stimulus position in degrees in patients and healthy participants (HP). The four stimuli were symmetrically positioned in the four quadrants.

Patient	Stimulus position (°)	
	X	Y
LF	12.2°	6.4°
AP	5.7°	11°
RC	8.6°	8°
BC	9°	3°
GS	4°	6.5°
LC	14°	3.3°
FB	13.8°	6.3°
HE	10.2°	8°
GA	7.3°	2.7°
SL	4.8°	4.8°
AN	13°	7.8°
LB	7.7°	7°
AM	5°	5°
HP[a]	5°	5°

[a] Healthy participants.

compared with the group of 13 healthy participants. An ANOVA was performed to analyse the power of frequency at 12 Hz in parieto-occipital electrodes for each group independently. To do that, two clusters of four electrodes with the mean power of the right parieto-occipital (O2, PO4, PO8 and PO10) and left parieto-occipital (O1, PO3, PO7 and PO9) channels were formed. Statistical analyses were conducted considering hemisphere (parieto-occipital left/intact and parieto-occipital right/lesioned), hemifield (left/blind and right/sighted) and quadrant (upper field and lower field) as within-subjects factors.

Given the presence of a conspicuous prefrontal activity a further electrode cluster from Fp1 and Fp2 was analysed considering hemifield (left/blind and right/sighted) and quadrant (upper field and lower field) as within-subjects factors for each group independently. For the statistical analyses, the Greenhouse-Geisser epsilon was applied to correct the degrees of freedom of the F-distribution. Post-hoc analyses were performed using the Bonferroni correction.

2.5.3.2.2. Step 2: Difference between patients with a left or right hemispheric lesion. The purpose of this step was to assess the difference in the power of frequency at 12 Hz between two groups of patients with similar lesions in opposite hemispheres: patients with right lesion (n = 3; RC, GS and HE) and patients with left lesion (n = 3; SL, AN and LB). This subset of patients was selected according to the similarity in the brain lesion as shown by the RM images and the

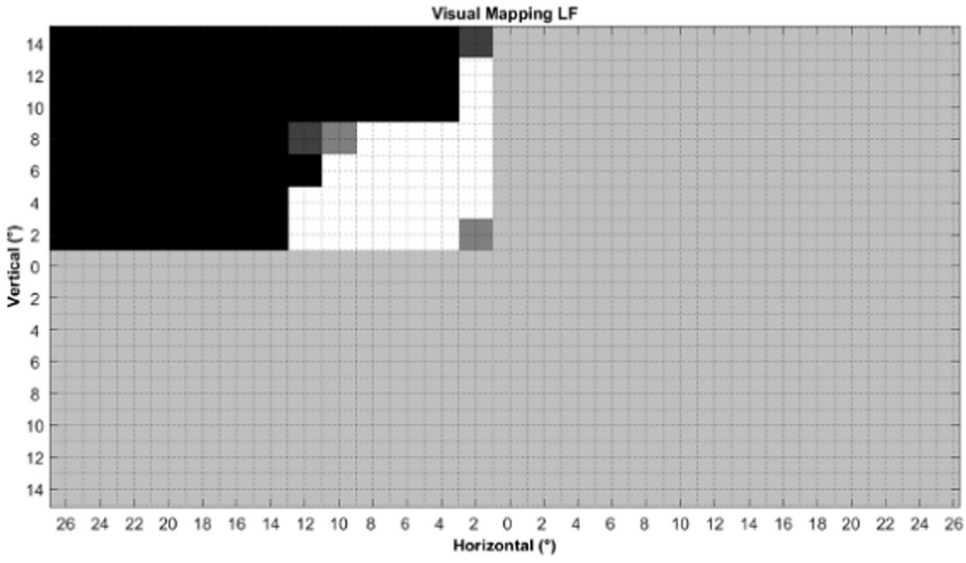

Fig. 4. Example of visual field mapping of patient LF (upper left quadrantanopia). Black squares indicate no responses (0/3), dark grey, grey and white indicates 1, 2 and 3 responses out of 3. Light grey in the lower left and right hemifields indicates the intact fields. Units on the vertical and horizontal axes are in degrees and each square on the grid represents 1° of visual angle at 57 cm from the screen.

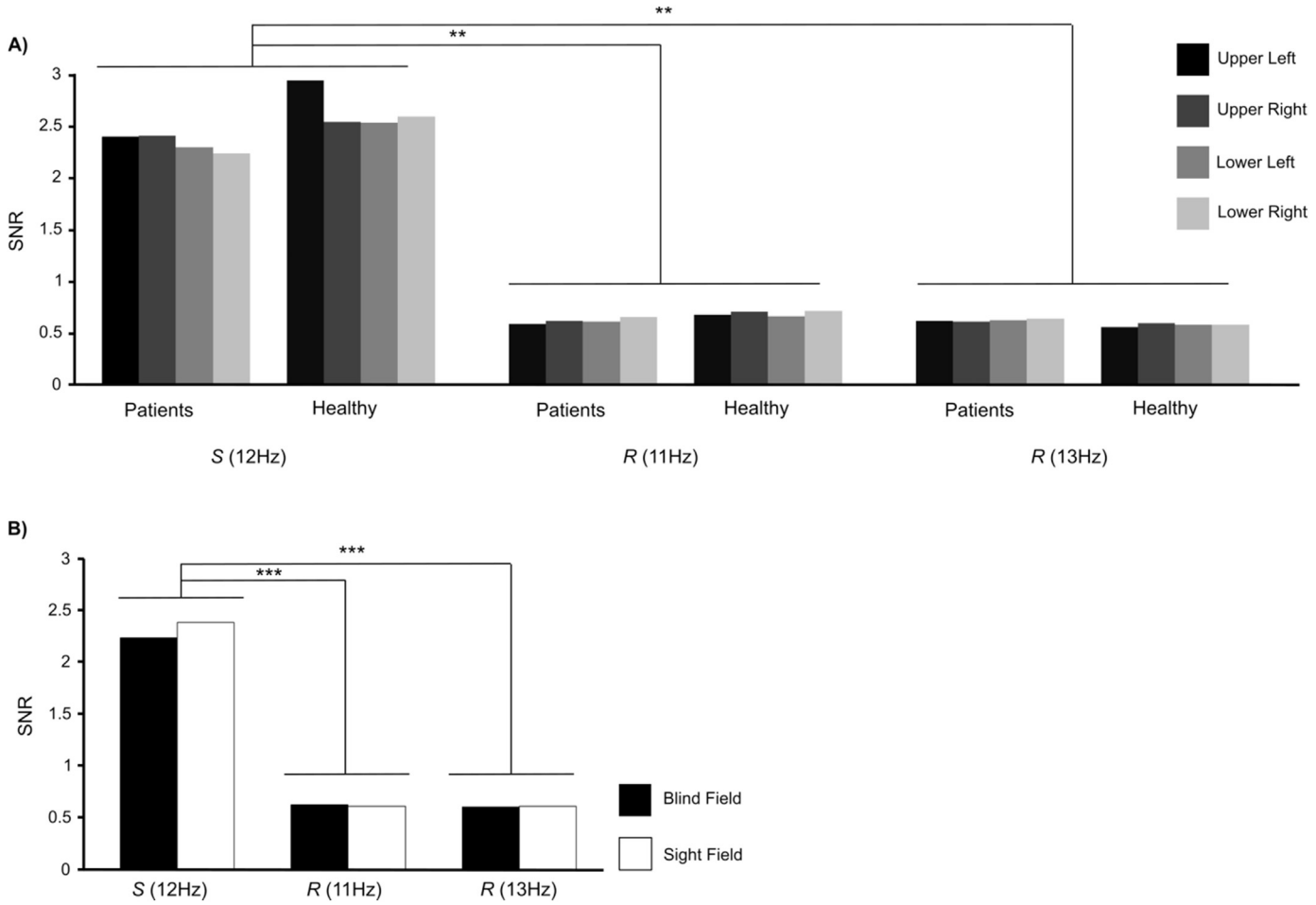

Fig. 5. SNR results for the patients group (A and B) and the healthy participants (A). Panel A shows the differences between *S* and *Rs* considering group (patients, n = 13; healthy participants, n = 13), quadrant (upper left, upper right, lower left, lower right) and frequency (12 Hz, 11 Hz, 13 Hz) as factors. Panel B shows the differences between *S* and *Rs* considering one blind and one intact fields in patients (n = 13) separately. ** $p < 0.01$, *** $p < 0.001$.

extension and location of the blind visual field documented by campimetry. Analyses consisted of a comparison between intact and damaged hemisphere of the clusters of parieto-occipital electrodes for each quadrant and group separately. The cluster of prefrontal electrodes was analysed by comparing quadrants (blind *vs* sighted) in each group and between groups (sighted *vs* sighted and blind *vs* blind). Considering group size, a non-parametric Monte Carlo Percentile Bootstrap Simulation (Efron and Tibshirani, 1993) was performed to assess the statistical differences. This method uses surrogate tests which consist of randomly re-sampling with replacement for 5000 times the data for each subject in the group to create a data distribution from the shuffled data with no normality assumptions.

2.5.3.2.3. Step 3: Difference between blind and sighted quadrants. For this last analysis, patients were grouped considering their blind and sighted quadrants: blind upper left (n = 9; LF, AP, RC, BC, GS, LC, FB, HE, AM), blind upper right (n = 4; SL, AN, LB, AM), blind lower left (n = 6; RC, BC, GS, LC, FB, HE), blind lower right (n = 4; GA, SL, AN, LB), sighted upper left (n = 4; GA, SL, AN, LB), sighted upper right (n = 9; LF, AP, RC, BC, GS, LC, FB, HE, GA), sighted lower left (n = 7; LF, AP, GA, SL, AN, LB, AM) and sighted lower right (n = 9; LF, AP, RC, BC, GS, LC, FB, HE, AM). Same non-parametric percentile Bootstrap re-sampling method (Efron and Tibshirani, 1993), described in Section 2.5.3.2.3, was used to explore statistical differences between left and right parieto-occipital cluster of electrodes for each condition and group separately. As in the Section 2.5.3.2.3, the cluster of frontal electrodes was analysed by comparing sighted and corresponding blind quadrants.

3. Results

3.1. Signal reliability

The SNR was calculated by means of the RESS method. Signal (*S* = 12 Hz) and references (*Rs* = 11 and 13 Hz) were extracted to make comparisons within and between subjects. An ANOVA showed no main effect of Group (patients *vs* healthy participants) ($F(1,24) = 2.05$, $p = 0.16$, $\eta_2 p = 0.07$). Incidentally, the lack of group differences justifies our decision to include a group of young healthy participants. Significant differences were observed in the main effect of Frequency ($F(2, 48) = 203.0$, $p < 0.001$, $\eta_2 p = 0.89$, $\varepsilon = 0.51$) with *S* significantly higher than *R* at 11 Hz (MD = 1.84) and *R* at 13 Hz (MD = 1.89). No other differences or interactions were observed.

In the **patients group** independent ANOVAs for blind and intact quadrants showed a significant effect of Frequency for both blind ($F(2, 24) = 378.31$, $p < 0.001$ $\eta_2 p = 0.969$) and intact ($F(2, 24) = 163.74$, $p < 0.001$, $\eta_2 p = 0.932$) hemifields. As in the previous analysis, *S* was higher than *Rs* for both blind ($MD_{11\ Hz} = 1.6$; $MD_{13\ Hz} = 1.6$) and intact ($MD_{11\ Hz} = 1.7$; $MD_{13\ Hz} = 1.7$) fields. Results are graphically represented in Fig. 5.

In sum, the important finding here was that the responses to blind field stimulation were significantly reliable as was the case for the intact hemifield of patients and for healthy participants. It is particularly reassuring that reliability was not different between patients and young healthy participants despite the substantial age difference.

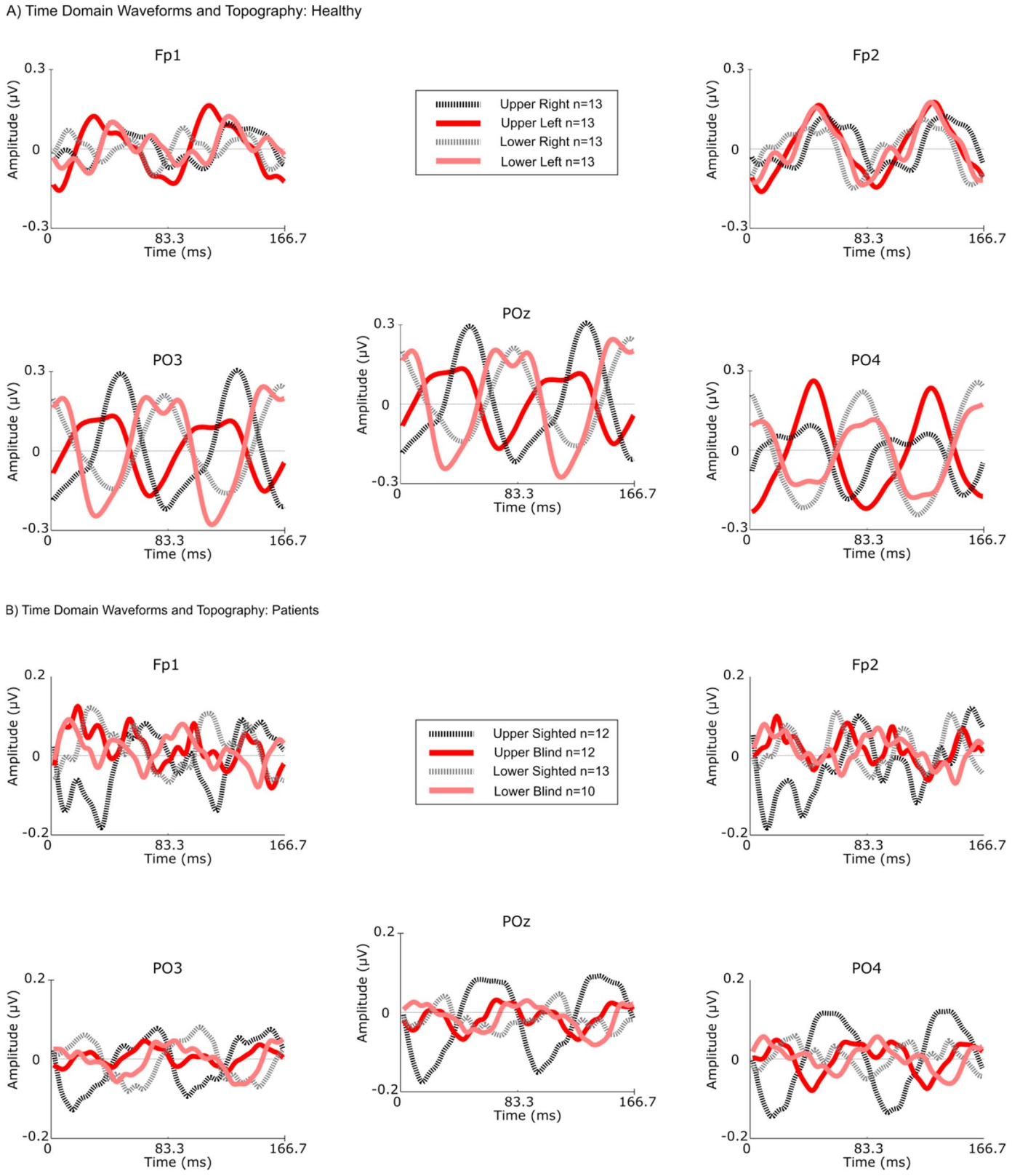

Fig. 6. Time SSVEP waveforms in healthy participants (A) and hemianopic patients (B). In the patients group, blind and sighted quadrants correspond to left and right visual field, respectively, as result of the left-right flipping. Positive values are plotted upward.

3.2. Time

Fig. 6 shows the time domain waveforms recorded from parieto-occipital and prefrontal electrodes for patients and healthy participants. Waveforms are represented in time windows of 166.7 ms corresponding to a complete cycle of pattern-reversal in the stimulation at 12 Hz

In the **healthy group**, waveforms were sinusoidally modulated at the frequency of stimulation (12 Hz). Interestingly, stimulus

presentation to the upper quadrants evoked higher amplitude waveforms than for the lower quadrants and this was similar to what described by Di Russo et al. (2007).

In the **patients group** some similarities with the healthy group were observed. First, even if of smaller amplitude, waveforms were sinusoidally modulated at 12 Hz across quadrants in either the blind or sighted field. Second, the spatio-temporal distribution for the upper blind and lower sighted field was similar to that of the healthy group. Third, the amplitude for the sighted upper field was higher than that for the lower sighted field.

However, there were **differences between patients and healthy participants** that concerned various parameters: First, the morphology of the waveforms was less defined in patients and their amplitude was smaller for both blind and sighted hemifields. Second, phase modulation (see Fig. 6A) in upper and lower fields of the healthy group was in antiphase (i.e. opposite phase of about 180° at POz electrode representing a normal pattern) while patients showed an abnormal antiphase pattern in the blind field (this was not the case for the intact field, see Fig. 6B).

3.3. Frequency

3.3.1. Step 1: General overview

As shown in Fig. 7A and B, in the **healthy group** the magnitude of the FFT in the power spectrum and in the topographical plotting was larger over the electrodes contralateral to the side of stimulation. This was not the case in the **patients group** (Fig. 7C and D) where this was only found for stimulation in the lower sighted and upper blind fields.

Topographic maps at 12 Hz in **healthy participants** (Fig. 7B) showed a focused activity in parieto-occipital scalp areas contralateral to the stimulated quadrant as well as a medial parieto-occipital activity (in keeping with the striate and extrastriate origin of SSVEP). In addition to this typical posterior activity, a strong medial prefrontal activity was present for all quadrants with a similar magnitude.

In the **patients group** (Fig. 7D), the parieto-occipital focus was more visible for sighted fields (especially for the lower), but was also detectable for the blind fields (especially for the upper). The medial prefrontal focus was also clearly present and stronger in the sighted fields.

In the **healthy group** an ANOVA on the parieto-occipital clusters showed a significant hemifield by hemisphere interaction ($F(1,12) = 7.98$, $p < 0.01$, $\eta_2 p = 0.40$). Post hoc analysis showed higher magnitude of power in the hemisphere contralateral to the stimulation side for both left (MD = 0.04, p = 0.01) and right (MD = 0.07, p = 0.04) visual fields.

In the **patients group** a significant hemifield by quadrant interaction was found ($F(1,8) = 7.91$, $p < 0.02$, $\eta_2 p = 0.49$), with the power of magnitude for the lower sighted visual field higher than for the lower blind visual field.

An ANOVA for the frontal electrodes, considering hemifield (left/blind and right/sighted) and quadrant (upper field and lower field) as factors, showed no significant differences either in the healthy or in the patients group. No other differences were found.

3.3.2. Step 2: Difference between patients with a right or left hemispheric lesion

Fig. 8 shows the FFT topographic maps of patients with right or left lesion. Two are the main differences observed by visual inspection: First, in the left group there is a higher power for stimuli presented to the sighted than to the blind hemifield; Second, in the left group, the focus of activity in posterior areas is mainly in the contralateral hemisphere (for upper left, upper right and lower left quadrants) while in the right group activity is less focused.

Importantly, the prefrontal activity is stronger in the sighted quadrants in comparison with the blind quadrants in both groups, but this is more pronounced in the left lesioned group.

Bootstrap statistical analysis showed significant differences only between left and right **parieto-occipital clusters** for the stimulation in the lower sighted-left hemifield in the left lesioned patients where the right cluster's magnitude (contralateral to the stimulation) was higher than left cluster (ipsilateral to the stimulation) (CI = 0.002, $p < 0.001$).

Statistical analyses over the **prefrontal cluster** concerned firstly the comparisons between sighted and blind upper or lower quadrants separately for each group. Results showed significant differences between the upper left sighted and upper right blind (CI = 0.07, $p < 0.001$) and between the lower left sighted and the lower right blind (CI = 0.07, $p < 0.001$) visual fields in the left lesioned patients group. In contrast, no significant differences were observed in the group of patients with right lesion.

Between-groups comparisons showed differences in the sighted lower fields between left lesioned and right lesioned patients (CI = 0.008, $p < 0.001$) where the magnitude of power was higher in the left lesioned group. No differences were observed between upper sighted fields or between blind upper or lower visual fields.

3.3.3. Step 3: Difference between blind and sighted quadrants

Fig. 9 shows SSVEP maps for blind and sighted hemifields. Occipital contralateral activity can be observed in the upper while it is missing in the lower blind quadrants where is visible a bilateral frontal-central activity. Sighted quadrants showed contralateral occipital activity for left stimulation while bilateral and ipsilateral activity was observed for upper right and lower right quadrants.

As reported for the FFT maps, a strong frontal activity was more prominent in sighted than blind quadrants. Comparisons between sighted and blind quadrants for the prefrontal cluster showed significantly higher frequency magnitude in the upper left sighted than in the left blind quadrant (CI = 0.0005, p = 0.05). Statistical analysis of the parieto-occipital clusters showed no significant differences (CI < 0, $p > 0.05$) between left and right hemisphere across quadrants in both blind and sighted hemifields. No other significant differences were observed.

4. Discussion

Most of the previous VEPs studies have found no reliable neural responses when hemianopic patients are visually stimulated in the blind visual field with transient stationary stimuli (Ffytche et al., 1996; Kavcic et al., 2015). More promising have been studies with moving stimuli especially in patients with above chance unconscious behavioural responses such as blindsight (Bollini et al., 2017; Ffytche et al., 1996) or some kind of residual visual awareness (see Mazzi et al. in this issue). In the light of this rather scanty evidence, the aim of the present study was to evaluate if SSVEPs elicited by stimulation of the blind (and intact) field of hemianopic patients might be a reliable means to obtain visual neural responses. These might be very useful data for studying the neural correlates of visual unconscious processing in these patients.

To achieve that, the first step adopted was assessing the SNR indices in both damaged and intact hemispheres for stimulus presentation to either intact or blind visual field quadrants, and comparing these data with those of healthy participants. We showed for the first time that the blind hemifield of hemianopic patients responds reliably to SSVEP stimulation independently from type of lesion and position of the visual field loss. This finding is clearly supported by the lack of difference in the SNR index between patients and controls and in the former between intact and blind visual hemifield.

Our results demonstrate that cortical blindness does not necessarily mean the absence of brain response in visual areas, especially when the lesion is restricted to visual primary areas (V1). One obvious, important question concerns what cerebral areas might subserve the neural responses from the blind field. fMRI studies have demonstrated some degree of brain reorganization in hemianopic patients that is likely to involve the vicarious functioning of other visual cortical areas such as

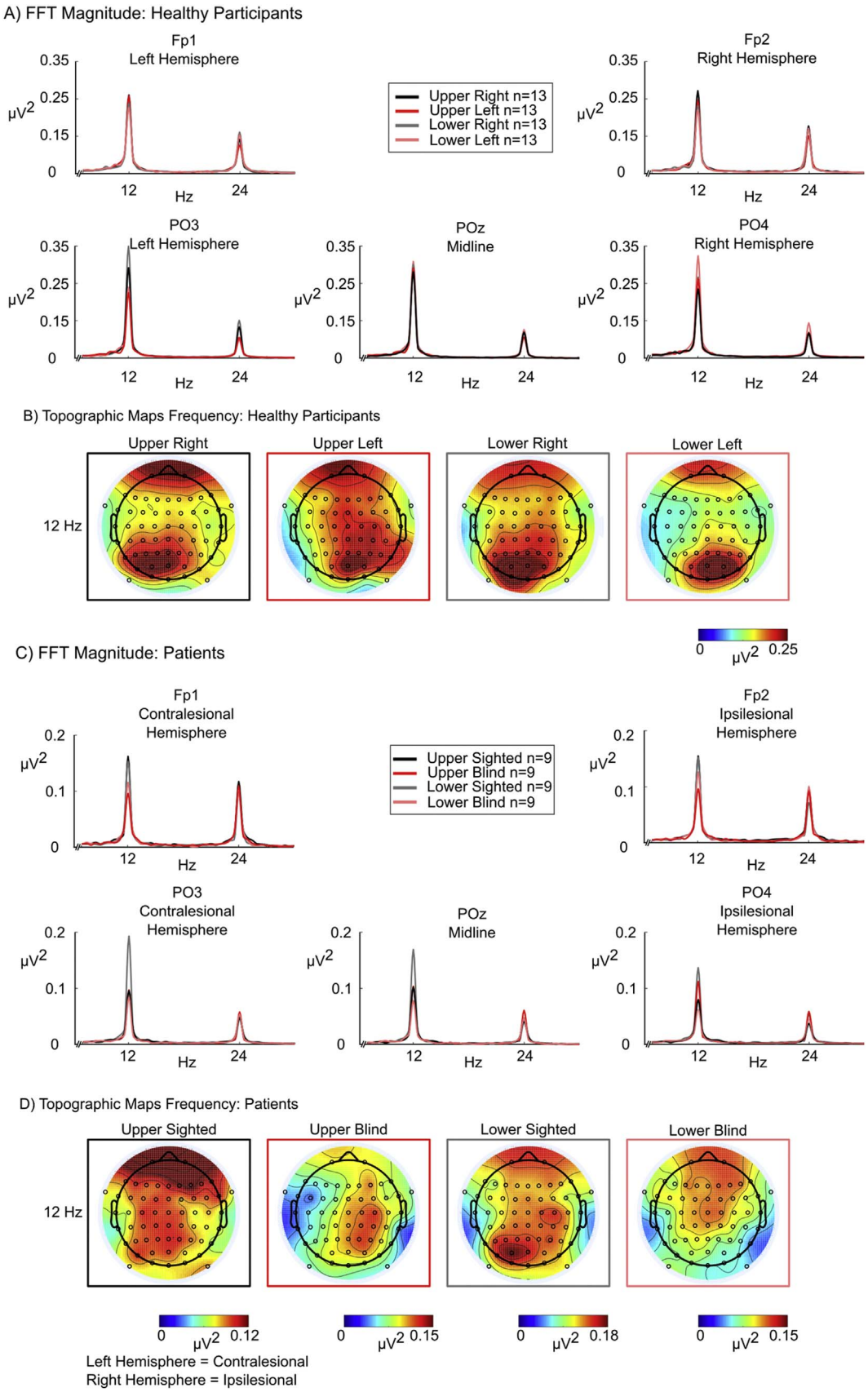

Fig. 7. Frequency modulation for patients and healthy participants. Panels A and C show the magnitude of the FFT at 12 Hz (frequency of stimulation) over parieto-occipital and prefrontal electrodes. In panels B and D are shown the scalp 2D circular flat topographic maps where the distribution of the power of frequency is represented for healthy participants and patients respectively. Topographic map scales in the patients group have been adjusted according to the maximum magnitude of frequency for each quadrant.

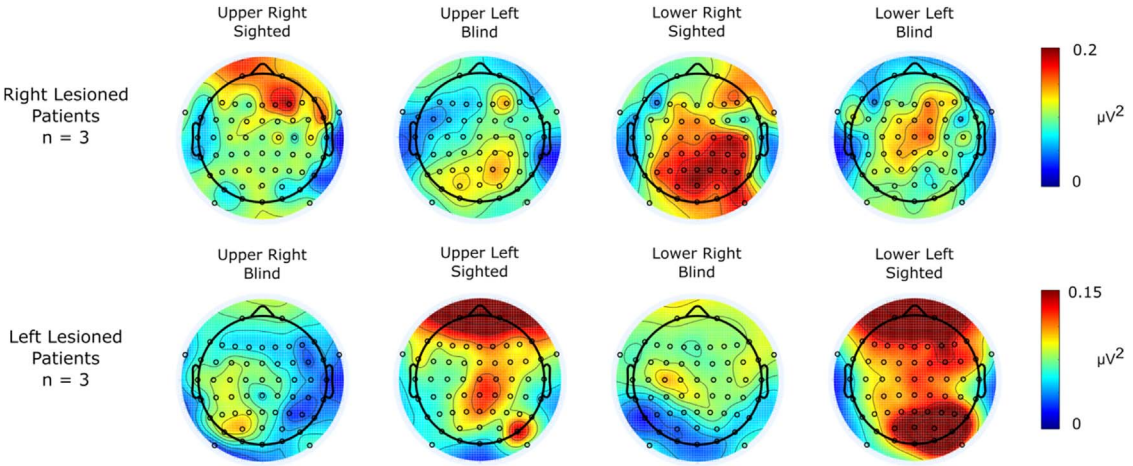

Fig. 8. Scalp 2D circular flat topographic maps of the magnitude of frequency at 12 Hz for right lesioned (top) and left lesioned (bottom) patients.

primarily the extrastriate visual cortex (Ajina et al., 2015; Bertini et al., 2017; Bridge et al., 2010; Nelles et al., 2007; Papanikolaou et al., 2014; Pitzalis et al., 2012). In particular it is known that the motion sensitive MT+ complex (or V5) receives direct input from subcortical areas such as the lateral geniculate nucleus (Ajina et al., 2015; Sincich et al., 2004), the pulvinar nuclei (Berman and Wurtz, 2010) and the superior colliculus (Gross, 1991). Furthermore, the existence of visual input to MT+ that bypass V1 has been also shown by means of transient VEP studies using motion-onset stimuli (Ffytche et al., 1996; Pitzalis et al., 2012). These are all likely possible neural substrates for the responses found for blind field stimulus presentation; in the present study we found SSVEP responses from the blind field broadly similar to those observed in previous studies with healthy participants (Di Russo et al., 2007). Since those studies have demonstrated the contribution of several extrastriate visual areas (V2, V3, V4/V8 and V5/MT+) in addition to V1 (Di Russo et al., 2007; Vialatte et al., 2010) to SSVEP responses in healthy participants, it is reasonable to expect similar sources in our hemianopics group.

All that said, one should point out that even if we found a reliable brain electrical activity following stimulus presentation to the blind field, this was qualitatively and quantitatively different from that in healthy participants for both intact and damaged hemisphere. Of course, one might wonder whether the group differences in the topographic distribution of the evoked activity might have been related not only to the brain lesion but also to the age of the patient group. In order to try and test for an age effect in the patients' responses we carried out a correlational analysis between age and magnitude of power evoked by stimulation of each single quadrant. This analysis was justified considering the large age range (47–75 years) of patients. No reliable correlations were observed, ($rho < 0.4$; $p > 0.05$). Even though this result is not directly relevant to the question it shows that an age difference of about 30 years does not result in a reliable power difference for the four visual quadrants.

As to the **parieto-occipital activity**, the main differences with respect to healthy participants were related to the amplitude and morphology of the SSVEP components in the time domain and to the topographical distribution in the frequency domain. Previous studies using current source localization analysis have identified V1 as the major cortical generator of the SSVEP signal (Di Russo et al., 2007; Lauritzen et al., 2010). Therefore, it is likely that the morphology and amplitude differences for stimulus presentation to the blind field depend on damage to V1. Interestingly, in the patients group there was no significant difference between the magnitude of power in the contralateral and ipsilateral hemisphere for the four quadrants as shown by visual inspection of the topographical distribution of the activity for stimulation in the blind fields (see Fig. 7D). This is not the case for the sighted field where magnitude of power was more similar to that of healthy participants (see Fig. 7B and D).

Moreover, the SSVEP phase in patients was abnormal for the blind field while it looked normal in the sighted field. Importantly, while the

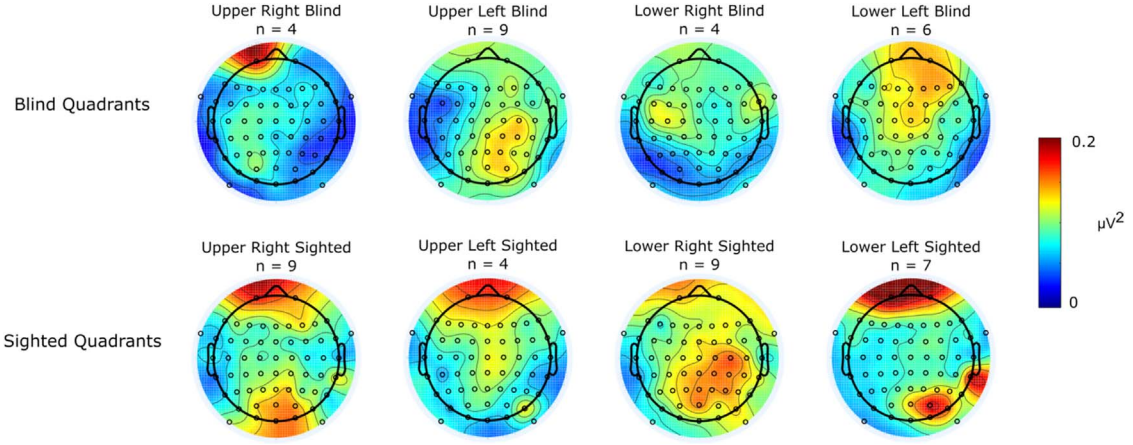

Fig. 9. Scalp 2D circular flat topographic maps of the magnitude of frequency at 12 Hz for blind (top) and sighted (bottom) quadrants.

SSVEP phase in healthy participants and the intact field of patients followed a pattern similar to the C1 ERP component (i.e. opposite phase between upper and lower visual fields) which is explained by the fact that C1 arises from neural generators in V1 (Di Russo et al., 2002a) this was not the case for the blind field.

In sum, SSVEP waveforms morphology and amplitude, magnitude of frequency power, topographical distribution and phase support the idea that the main contribution to the SSVEP activity recorded from the blind field is mainly from extrastriate cortical areas bypassing V1 as proposed in neuroimaging (Bridge et al., 2010; Nelles et al., 2007; Papanikolaou et al., 2014) and transient VEP (Ffytche et al., 1996; Schoenfeld et al., 2002) studies, as well as in a study combining VEP and fMRI and including detailed retinotopic analyses (Pitzalis et al., 2012).

In addition to the posterior parietal-occipital activity, a strong **medial prefrontal activity** was observed in both patients and healthy participants (see subsection 3.2 and 3.3). This anterior activity was present for the sighted hemifield of hemianopic patients and was similar to that observed in healthy participants. In contrast, there was a lack (or strong reduction) of this activity in the blind hemifield. This is in keeping with recent findings showing that early ERP components recorded from prefrontal electrodes are related to visual processing. In particular the pN1 and pP1 are concomitant to the parieto-occipital P1 and N1components at about 100 and 180 ms and are related to stimulus appearance while the pP2 is concomitant to N2 (about 300 ms) and has been associated to processing of target stimuli (Berchicci et al., 2016; Di Russo et al., 2016; Perri et al., in press). Studies combining ERP and fMRI found that the source of these prefrontal ERPs is the rostral part of the anterior insula (Di Russo et al., 2016; Sulpizio et al., 2017). The pN1, which is also present for passive stimulation (Di Rollo et al., 2016; Perri et al., unpublished; Zeri et al., unpublished), has been suggested to be related to the emergence of perceptual awareness (Passingham and Lau, 2017). The lack of this early insular activity for the blind hemifield of hemianopics thus, fits in with the lack of perceptual awareness in these patients.

Several previous studies have found that the intact visual field in patients with retrochiasmatic lesions might not be completely normal. Deficits of spatial, temporal (Hess and Pointer, 1989) and contrast sensitivity (Clatworthy et al., 2013), impaired signal detection (Paramei and Sabel, 2008) and deficits in early and late visual processing of Gestalt stimuli (Schadow et al., 2009) have been observed. These deficits in the sighted field of hemianopics are characterized by differences in cortical activation between left and right lesioned patients (Cavézian et al., 2015). In our study, for stimulation of the intact field we found a widespread bilateral activity in right-lesioned patients and contralateral activity in left-lesioned patients (see subsection 3.3.2). Similar results were also observed when patients were grouped according to their sighted quadrants (see Section 3.3.3). These results are consistent with those of Perez et al. (2013), and corroborate the hypothesis that the side of the occipital lesion is relevant for the cortical reorganization enabling functional recovery. From our results it follows that this reorganization may also affect the basal state of the visual system during passive stimulation and not only during task performance.

In conclusion, our results demonstrate the effectiveness of SSVEP in the study of the visual function in patients with retrochiasmatic lesions; they also suggest different patterns of reorganization depending on the side of lesion and the role of the anterior insula in perceptual awareness. SSVEP technique promises to be a good approach to the study of more complex processes in hemianopic patients (e.g. attention and memory) and in the assessment of different levels of visual consciousness. Furthermore, SSVEP is likely to result as a very valuable objective tool to establish the presence of visual neural responses in cortical blindness and to predict the feasibility of a rehabilitation procedure. This is in broad keeping with what has been proposed for the pupillary response to light (Sahraie et al., 2013; see also Binda and Gamlin, 2017 and Ebitz and Moore, 2017). In the present study we did not attempt to correlate SSVEP responses and presence of blindsight type I or II and therefore we cannot demonstrate the feasibility of this method to predict blindsight or a successful outcome of visual rehabilitation but we are confident that future studies will cast light on this important possibility.

Funding

The study was supported by the European Research Council (ERC) Grant number 339939 “Perceptual Awareness” (P.I.: C.A. Marzi)

References

Ajina, S., Pestilli, F., Rokem, A., Kennard, C., Bridge, H., 2015. Human blindsight is mediated by an intact geniculo-extrastriate pathway. Elife 4, 1–23. http://dx.doi.org/10.7554/eLife.08935.

Berchicci, M., Spinelli, D., Di Russo, F., 2016. New insights into old waves. Matching stimulus- and response-locked ERPs on the same time-window. Biol. Psychol. 117, 202–215. http://dx.doi.org/10.1016/j.biopsycho.2016.04.007.

Berman, R.A., Wurtz, R., 2010. Functional identification of a pulvinar path from superior colliculus to cortical area MT. J. Neurosci. 30, 6342–6354. http://dx.doi.org/10.1523/JNEUROSCI.6176-09.2010.

Bertini, C., Cecere, R., Làdavas, E., 2017. Unseen fearful faces facilitate visual discrimination in the intact field. Neuropsychologia. http://dx.doi.org/10.1016/j.neuropsychologia.2017.07.029.

Binda, P., Gamlin, P.D., 2017. Renewed attention on the pupil light reflex. Trends Neurosci. 40, 455–457. http://dx.doi.org/10.1016/j.tins.2017.06.007.

Bollini, A., Sanchez-Lopez, J., Savazzi, S., Marzi, C.A., 2017. Lights from the dark: neural responses from a blind visual hemifield. Front. Neurosci. 11. http://dx.doi.org/10.3389/fnins.2017.00290.

Bouwmeester, L., Heutink, J., Lucas, C., 2007. The effect of visual training for patients with visual field defects due to brain damage: a systematic review. J. Neurol. Neurosurg. Psychiatry 78, 555–564. http://dx.doi.org/10.1136/jnnp.2006.103853.

Brecelj, J., 1991. E 114–122.

Bridge, H., Hicks, S.L., Xie, J., Okell, T.W., Mannan, S., Alexander, I., Cowey, A., Kennard, C., 2010. Visual activation of extra-striate cortex in the absence of V1 activation. Neuropsychologia 48, 4148–4154. http://dx.doi.org/10.1016/j.neuropsychologia.2010.10.022.

Cavézian, C., Perez, C., Peyrin, C., Gaudry, I., Obadia, M., Gout, O., Chokron, S., 2015. Hemisphere-dependent ipsilesional deficits in hemianopia: sightblindness in the “intact” visual field. Cortex 69, 166–174. http://dx.doi.org/10.1016/j.cortex.2015.05.010.

Celesia, G.G., Brigell, M.G., 1999. Cortical blindness and visual processing. Electroencephalogr. Clin. Neurophysiol. Suppl. 49, 133–141.

Clatworthy, P.L., Warburton, E.A., Tolhurst, D.J., Baron, J.C., 2013. Visual contrast sensitivity deficits in “normal” visual field of patients with homonymous visual field defects due to stroke: a pilot study. Cerebrovasc. Dis. 36, 329–335. http://dx.doi.org/10.1159/000354810.

Cohen, M.X., Gulbinaite, R., 2017. Rhythmic entrainment source separation: optimizing analyses of neural responses to rhythmic sensory stimulation. Neuroimage 147, 43–56. http://dx.doi.org/10.1016/j.neuroimage.2016.11.036.

Delorme, A., Makeig, S., 2004. EEGLAB: an open source toolbox for analysis of single-trial EEG dynamics including independent component analysis. J. Neurosci. Methods 134, 9–21. http://dx.doi.org/10.1016/j.jneumeth.2003.10.009.

Di Rollo, A., Cosottini, M., Pesaresi, I., Fabbri, S., Di Russo, F., Perri, R.L., Barloscio, D., Bocci, T., Ragazzoni, A., Sartucci, F., 2016. 29. ERP generators in an omitted-target oddball task: a simultaneous EEG-fMRI study. Clin. Neurophysiol. 127, e330. http://dx.doi.org/10.1016/j.clinph.2016.10.041.

Di Russo, F., Lucci, G., Sulpizio, V., Berchicci, M., Spinelli, D., Pitzalis, S., Galati, G., 2016. Spatiotemporal brain mapping during preparation, perception, and action. Neuroimage 126, 1–14. http://dx.doi.org/10.1016/j.neuroimage.2015.11.036.

Di Russo, F., Martínez, A., Sereno, M.I., Pitzalis, S., Hillyard, S.A., 2002a. Cortical sources of the early components of the visual evoked potential. Hum. Brain Mapp. 15, 95–111. http://dx.doi.org/10.1002/hbm.10010.

Di Russo, F., Pitzalis, S., Aprile, T., Spitoni, G., Patria, F., Stella, A., Spinelli, D., Hillyard, S.A., 2007. Spatiotemporal analysis of the cortical sources of the steady-state visual evoked potential. Hum. Brain Mapp. 28, 323–334. http://dx.doi.org/10.1002/hbm.20276.

Di Russo, F., Teder-Sälejärvi, W.A., Hillyard, S.A., 2002b. Steady-state VEP and attentional visual processing. Cogn. Electrophysiol. Mind Brain 11, 257–272.

Diller, L., Ben-Yishay, Y., Gerstman, L., 1974. Studies in Cognition and Rehabilitation In

Hemiplegia. New York University Medical Center Institute of Rehabilitation Medicine, New York.
Ebitz, R.B., Moore, T., 2017. Selective modulation of the pupil light reflex by microstimulation of prefrontal cortex. J. Neurosci. 37, 5008–5018. http://dx.doi.org/10.1523/JNEUROSCI.2433-16.2017.
Efron, B., Tibshirani, R.J., 1993. An Introduction to the Bootstrap. Chapman Hall, New York.
Ffytche, D.H., Guy, C.N., Zeki, S., 1996. Motion specific responses from a blind hemifield. Brain 119, 1971–1982. http://dx.doi.org/10.1093/brain/119.6.1971.
Folstein, M.F., Folstein, S.E., McHugh, P.R., 1975. "Mini-mental state". A practical method for grading the cognitive state of patients for the clinician. J. Psychiatr. Res. 12, 189–198. http://dx.doi.org/10.1016/0022-3956(75)90026-6.
Gauthier, L., Dehaut, F., Joanette, Y., 1989. The Bells test: a quantitative and qualitative test for visual neglect. Int. J. Clin. Neuropsychol.
Gross, C.G., 1991. Contribution of striate cortex and the to visual function in area MT, the superior temporal polysensory area and inferior temporal cortex. Neuropsychologia 29, 497–515.
Hess, R.F., Pointer, J.S., 1989. Spatial and temporal contrast sensitivity in hemianopia. Brain 112, 871–894.
Kavcic, V., Triplett, R.L., Das, A., Martin, T., Huxlin, K.R., 2015. Role of inter-hemispheric transfer in generating visual evoked potentials in V1-damaged brain hemispheres. Neuropsychologia 68, 82–93. http://dx.doi.org/10.1016/j.neuropsychologia.2015.01.003.
Lauritzen, T.Z., Ales, J.M., Wade, A.R., 2010. The effects of visuospatial attention measured across visual cortex using source-imaged, steady-state EEG. J. Vis. 10, 1–17. http://dx.doi.org/10.1167/10.14.39.
Makeig, S., Bell, J., Jung, A., Sejnowski, T.J, T.-P., 1996. Independent component analysis of electroencephalographic data. Adv. Neural Inf. Process. Syst. 8, 145–151. http://dx.doi.org/10.1109/ICOSP.2002.1180091.
Mangione, C.M., Lee, P.P., Gutierrez, P.R., Spritzer, K., Berry, S., Hays, R.D., National Eye Institute Visual Function Questionnaire Field Test Investigators, 2001. Development of the 25-item national eye institute visual function questionnaire. Arch. Ophthalmol. 119, 1050–1058. http://dx.doi.org/10.1097/00132578-200201000-00028. (Chicago, Ill. 1960).
Mazzi, C., Tagliabue, C.F., Mazzeo, G., Savazzi, S., n.d. Reliability in reporting perceptual experience: behaviour and electrophysiology in hemianopic patients (in this issue).
Nelles, G., de Greiff, A., Pscherer, A., Forsting, M., Gerhard, H., Esser, J., Diener, H.C., 2007. Cortical activation in hemianopia after stroke. Neurosci. Lett. 426, 34–38. http://dx.doi.org/10.1016/j.neulet.2007.08.028.
Papanikolaou, A., Keliris, G.A., Papageorgiou, T.D., Shao, Y., Krapp, E., Papageorgiou, E., Stingl, K., Bruckmann, A., Schiefer, U., Logothetis, N.K., Smirnakis, S.M., 2014. Population receptive field analysis of the primary visual cortex complements perimetry in patients with homonymous visual field defects. Proc. Natl. Acad. Sci. USA 111, E1656–E1665. http://dx.doi.org/10.1073/pnas.1317074111.
Paramei, G.V., Sabel, B.A., 2008. Contour-integration deficits on the intact side of the visual field in hemianopia patients. Behav. Brain Res. 188, 109–124. http://dx.doi.org/10.1016/j.bbr.2007.10.025.
Passingham, R.E., Lau, H.C., 2017. Acting, seeing, and conscious awareness. Neuropsychologia. http://dx.doi.org/10.1016/j.neuropsychologia.2017.06.012.
Perez, C., Peyrin, C., Cavézian, C., Coubard, O., Caetta, F., Raz, N., Levin, N., Doucet, G., Andersson, F., Obadia, M., Gout, O., Héran, F., Savatovsky, J., Chokron, S., 2013. An fMRI investigation of the cortical network underlying detection and categorization abilities in hemianopic patients. Brain Topogr. 26, 264–277. http://dx.doi.org/10.1007/s10548-012-0244-z.
Perri, R.L., Berchicci, M., Bianco, V., Quinzi, F., Spinelli, D., Di Russo, F., n.d. Endogenous Visual Processing Associated with Perceptual Analysis within the Anterior Insula (unpublished).
Perri, R.L., Berchicci, M., Bianco, V., Spinelli, D., Di Russo, F., 2017. Brain waves from an "isolated" cortex: Contribution of the anterior insula to cognitive functions. Brain Struct. Funct (in press).
Pitzalis, S., Strappini, F., de Gasperis, M., Bultrini, A., Di Russo, F., 2012. Spatio-temporal brain mapping of motion-onset VEPs combined with fMRI and retinotopic maps. PLoS One 7. http://dx.doi.org/10.1371/journal.pone.0035771.
Poppel, E., Held, R., Frost, D., 1973. Residual visual function after brain wounds involving the central visual pathways in man. Nature 243, 295–296.
Regan, D., 1989. Human Brain Electrophysiology. Evoked Potentials And Evoked Magnetic Fields in Science and Medicine, Electroencephalography and Clinical Neurophysiology. Elsevier, New York.
Rossion, B., De Gelder, B., Pourtois, G., Guérit, J.M., Weiskrantz, L., 2000. Early extrastriate activity without primary visual cortex in humans. Neurosci. Lett. 279, 25–28. http://dx.doi.org/10.1016/S0304-3940(99)00926-X.
Sahraie, A., Trevethan, C.T., MacLeod, M.J., Urquhart, J., Weiskrantz, L., 2013. Pupil response as a predictor of blindsight in hemianopia. Proc. Natl. Acad. Sci. USA 110, 18333–18338. http://dx.doi.org/10.1073/pnas.1318395110.
Schadow, J., Dettler, N., Paramei, G.V., Lenz, D., Fründ, I., Sabel, B.A., Herrmann, C.S., 2009. Impairments of Gestalt perception in the intact hemifield of hemianopic patients are reflected in gamma-band EEG activity. Neuropsychologia 47, 556–568. http://dx.doi.org/10.1016/j.neuropsychologia.2008.10.012.
Schenkenberg, T., Bradford, D.C., Ajax, E.T., 1980. Line bisection and unilateral visual neglect in patients with neurologic impairment (509–509). Neurology 30. http://dx.doi.org/10.1212/WNL.30.5.509.
Schoenfeld, M.A., Heinze, H.J., Woldorff, M.G., 2002. Unmasking motion-processing activity in human brain area V5/MT+ mediated by pathways that bypass primary visual cortex. Neuroimage 17, 769–779. http://dx.doi.org/10.1016/S1053-8119(02)91204-8.
Schomer, D.L., Lopes da Silva, F.H., 2011. Niedermeyer's Electroencephalography, sixth. ed. Wolters Kluwer Health/Lippincott Williams & Wilkins.
Shefrin, S.L., Goodin, D.S., Aminoff, M.J., 1988. Visual evoked potentials in the investigation of "blindsight". Neurology 38, 104–109.
Sincich, L.L.C., Park, K.F.K., Wohlgemuth, M.J.M., Horton, J.C.J., 2004. Bypassing V1: a direct geniculate input to area MT. Nat. Neurosci. 7, 1123–1128. http://dx.doi.org/10.1038/nn1318.
Sulpizio, V., Lucci, G., Berchicci, M., Galati, G., Pitzalis, S., Di Russo, F., 2017. Hemispheric asymmetries in the transition from action preparation to execution. Neuroimage 148, 390–402. http://dx.doi.org/10.1016/j.neuroimage.2017.01.009.
Vialatte, F.B., Maurice, M., Dauwels, J., Cichocki, A., 2010. Steady-state visually evoked potentials: focus on essential paradigms and future perspectives. Prog. Neurobiol. http://dx.doi.org/10.1016/j.pneurobio.2009.11.005.
Weiskrantz, L., 1997. Consciousness Lost and Found: a Neuropsychological Exploration. Oxford University Press, New York.
Weiskrantz, L., 1996. Blindsight revisited. Curr. Opin. Neurobiol. 6, 215–220. http://dx.doi.org/10.1016/S0959-4388(96)80075-4.
Weiskrantz, L., Warrington, E.K., Sanders, M.D., Marshall, J., 1974. Visual capacity in the hemianopic field following a restricted occipital ablation. Brain 97, 709–728.
Zeri, F., Berchicci, M., Naroo, S., Pitzalis, P., Di Russo, F., n.d. Short -term visual cortical plasticity in visual and non-visual areas induced by monovision (unpublished).